UNIVERSIDADE DE SÃO PAULO

INSTITUTO DE FÍSICA
CAIXA POSTAL 20516
01000 - SÃO PAULO - SP
BRASIL

publicações

IFUSP/P-373

A STUDY OF POINT DEFECT AGGREGATES IN γ-IRRADIATED LiF SINGLE CRYSTALS

by

P.A. Frugoli and C.A. Pimentel
Instituto de Física, Universidade de São Paulo

Novembro/1982

A STUDY OF POINT DEFECT AGGREGATES IN γ-IRRADIATED LiF SINGLE CRYSTALS

P.A. Frugoli and C.A. Pimentel

Instituto de Física da Universidade de São Paulo
C. Postal 20.516, 05508 - São Paulo, Brasil

ABSTRACT

Diffuse X-ray scattering near the Bragg Reflection and Bragg profile analysis have been made in γ-irradiated LiF single crystals using a double crystal X-ray diffractometer. An estimate of the half-width of the diffraction patterns was done and a preferential alteration in the profile parameters was observed. Clusters with mean parameter sizes from hundreds to thousands of angstroms were observed but each sample has presented a set of average size values. The nature of clusters was found be dependent on the γ-dose: vacancy at low dose (~10 MRad) and interstitial at high dose (~50 MRad). Some process of coalescence at 50 MRad seems to occur.

RÉSUME

La diffusion des rayons X près des réflections de Bragg a été étudieé ainsi que le profil des raies des monocristaux de LiF γ-irradiés en employant un spectromètre à double cristaux. Les largeurs des profils de diffraction à mi-intensité ont été évalueés. Des changements préférentiels des paramètres du profil sont apparus. Des agrégats de dimension moyenne de cents à milles angströms sont observés, chaque échantillon présentant un ensemble de valeurs de dimension. Le type d'agrégats varie en relation de la γ-dose: lacune à basse dose (10 MRad), interstitiel à haute dose (50 MRad). Quelque procès de coalition semble se manifester à 50 MRad.

INTRODUCTION

The clustering processes of point defects in γ-irradiated LiF single crystals have being investigated on both theoretical and experimental approaches [1 to 3]. During irradiation, F centers and interstitial halogen atoms are simultaneously produced; at room temperature extended defects are formed due to mobility of these point defects [4 to 8]. Small aggregates of a well-defined size (10 Å) already exist at low irradiation doses (0.85 MRad); prolonged irradiations give rise to clusters of interstitial atoms of ca. 500 Å [7,9,10]. These large clusters (~300 Å for 80 MRad) which appear at doses of 10 MRad were identified with extended agglomerates of interstitial fluorine ions [8]. Clustering processes on (100) planes have been observed by Spalt [11]. The presence of point defects and their aggregates was also observed after γ-background irradiation (~50 MRad) in the reactor at room temperature, the crystalline planes being differently altered [12 to 15]. In spite of all efforts the detailed mechanism for interstitial aggregation in LiF γ-irradiated is still unknown [16]. Diffuse X-ray scattering analysis near the Bragg reflection (DXS) has been employed to characterize defects in irradiated alkaline halides [7,9,17 to 20,11,13,14,21]. This DXS technique has been developed into a very powerful toll for the investigation of the structure and size of defects [22 to 25]. In the present paper defects induced in LiF single crytals by γ-irradiation at room temperature are studied. The DXS in several lattice sites are analysed in order to characterize

the nature and size of the clusters and their dependence on the γ-doses. The profile of Bragg reflection (BLP) [12,13,21,26,27] is also analysed since its parameters can give information about how the crystalline planes are affected by irradiation processes. The widths at half height of the diffraction patterns of the irradiated samples are estimated.

OUTLINE OF THE METHOD

The basic theory of DXS from point defects and their aggregates has been discussed by several authors (for a review, 22 to 25). The DXS is analysed as a function of a vector $\vec{q}$ defined as the difference between the scattering vector $\vec{k}$ and the nearest reciprocal lattice vector $\vec{h}$: $\vec{q} = \vec{k} - \vec{h}$. The DXS intensity (I) follows the $1/q^2$ behaviour (Huang scattering) for a small q values and the $1/q^4$ behaviour (Stokes-Wilson scattering) for large q values. A cluster size R_{cr} can be estimated from the crossing point of the Huang and Stokes-Wilson scattering in a $\log I$ vs. $\log q$ plot. Another procedure to evaluate the parameter size R_o of the cluster from DXS intensity measured in a double-crystal spectrometer involves the consideration of I as a function of $q_o = q \cos\theta$ (θ , scattering angle); a plot of $I(q_o)$ vs. $\ell n\ q_o$ should be linear until a particular q_o value; the intercept ($I(q_o) = 0$) of this straight line with the horizontal q axis is $\simeq 1/R_o$. Lal and co-workers [28 to 30] have studied DXS from a $I(q)$ vs. $1/q^2$ plot where a straight line

is expected if the observed DXS corresponds to Huang scattering. Under experimental conditions of high resolution they have obtained for silicon single crystals two or more straight lines, with different slopes, defining the so-called knee points that can give information about the size of the clusters. Similar results were also obtained for doped silicon single crystals [26,27] and γ-irradiated LiF single crystals [21].

In order to study the DXS very near a Bragg reflection, accurate experimental conditions are required such as a highly collimated and monochromated X-ray beam [31,32,21, 26 to 28]. These same conditions are required for profile analysis of Bragg reflection which can give information about defects in single crystals, despite their lingering qualitative aspect for some defects [13,21,26,27]. In this paper the intensity measurements were carried out in a double-crystal X-ray diffractometer under high resolution conditions.

EXPERIMENTAL

The LiF samples - plates of 5x5x1 mm - were obtained by cleavage from a Harshaw single crystal which was X-ray irradiated to insure proper cleavage [33]. The samples were then annealed for 2 hours at 700°C followed by a slow cool-down (~20 hours) to room temperature. Irradiation damage was carried out in a ^{60}Co γ-source of 2.7×10^5 curies activity with γ-doses from 0.5 to 100 MRad at a temperature of about 30°C. A luminescent dosimeter was employed to

measure the γ-dose, within an error of 10% . The great penetration depth of the γ-rays has assured homogeneous coloration to the samples.

For DXS measurements a double crystal diffractometer was employed in a parallel arrangement, with a linear beam from a fine focus Cu tube; a Ge single crystal monochromator and a pinhole system were used to obtain $K\alpha_1$ radiation [26,27]. A scintillation counter and pulse-height analyser were used to detect the diffracted beam. A ω- or θ-scanning of the sample permitted the obtaining of the BLP in a plotter or by counting the intensity step to step with $\Delta\theta$ varying to as little as 2.5×10^{-4} degrees or less. The centralization of the samples in the X-ray diffractometer [12,13] is of fundamental importance for the BLP and DXS analysis. After an accurate optical alignment, the crystal is adjusted until the [200] scattering vector is exactly perpendicular to the θ-rotation axis. To avoid truncation errors in the BLP, the intensity was measured until the background counting was reached. The background was measured for several ω on both sides of each BLP; its correction was made by subtracting from each intensity value the correspondent background intensity obtained for each reflection, adjusting a straight line by the method of the least mean square.

In order to assure the homogeneity and perfection of the samples, the (200) BLP of all the crystals was analysed, the differences among its parameters being within experimental errors. During the experiment it was verified that the intensity of the exploring X-ray beam was constant; this unit

is thus the same for all BLP and DXS. In this paper, the intensity always refers to relative intensity in arbitrary unit.

RESULTS AND DISCUSSION

a) BRAGG LINE PROFILE ANALYSIS

Figure 1 and 2 show the variation of (hkℓ) Bragg profile parameters of LiF cyrstal for γ-irradiated doses from 0.5 to 100 MRad: peak intensity (PI), integrated intensity (II), width al half height (β) and integral width (B). The β parameter was measured directly on the BLP. A careful estimate of errors e was carried out, resulting for (111) and (200) reflections $e_{PI} \sim 0.5\%$ and $e_{II} \sim 1{,}5\%$ while for the other reflections, $e_{PI} \simeq e_{II} \simeq 1\%$, $e_\beta \simeq e_B \simeq 2\%$. The irradiation process has affected differently the BLP parameters and a complete interpretation of the observed variations for all reflections is not trivial. A general bahaviour of the BLP parameters will be taken into account in their analysis. Up to 10 MRad BLP parameters have not shown the marked alterations which occur particularly at 100 MRad. As a general tendency (Fig. 1a and b), PI and II tend to decrease with the increasing of the γ-dose while the opposite occurs for both B and β width (Fig. 2a and b). (These width parameters have shown similar behaviour since DXS intensity is not so large as to alter significantively B). This behaviour is related to the loss of crystalline perfection due to the introduction of defects.

BLP results put in evidence the preferential alterations suffered by crystalline planes due to irradiation process, particularly in (111) reflections, followed by (200). LiF single crystals irradiated with reactor γ-background [12,13] have also shown (111) reflection as the most altered by that irradiation process. In alkaline halogen a preferential migration of interstitials in <111> direction is theoretically expected [34], as well as a relaxation of the lattice in this crystalographic direction [35]. The marked and systematic increase of the half-width and integral intensity together with the reduction of PI expresses the increase of internal stress in the heavily γ-irradiated LiF single crystals, particularly affecting (111) planes.

At 50 MRad PI tends to increase and II, B and β tend to decrease. The most affected reflection is (200) which presents the largest alterations in II and width parameters. From the general behavior of BLP parameters the sample seems at this γ-dose to require part of its crystalline perfection, lost by the irradiation process. This could be understood if some defect aggregation processes are intensified at this dose; the crystal could then present large regions less stressed and more perfect. The increase of γ-dose from 50 to 100 MRad and the consequent introduction of a higher number of defects affect the partially restored crystalline perfection, broadening the Bragg profile.

b) DIFFRACTION PATTERN HALF WIDTH (An Estimate)

Another analysis of the β parameter may be

done taking explicitly into account the broadening due to dispersion. For an expected broadening $\Delta\theta = \Delta\lambda/2d \cos\theta$, the variation of β with the increasing of $1/\cos\theta$ is shown in Fig. 3a. In this experimental condition, $\beta = \beta^* + |D|\Delta\lambda$, where β^* refers to the BLP resulted from the convolution of pattern diffractions (of half-widths β_{Ge} and β_{LiF}) of the first (Ge) and second (LiF) crystals. The term $|D|\Delta\lambda$ is due to instrumental dispersion, where $\Delta\lambda$ is the width of X-ray spectral line (Cu $K\alpha_1$) and $|D| = |\mathrm{tg}\ \theta_{Ge\ 111} - \mathrm{tg}\ \theta_{LiF\ hk\ell}|$ [26]. Fig. 3b shows this other procedure used to analyse the contribution of dispersion. For the less irradiated sample, both procedures allow a rather good fitting of a straight line despite the presence of defects, certainly introduced by irradiation. At a condition of null dispersion, β has practically the value of the most narrow diffraction pattern; in the present case, $\beta \simeq \beta_{Ge\ 111} = 11'$ which is the value of the linear coefficient from the plot of Fig. 3b. In this plot, the angular coefficient of the straight line, $\Delta\lambda/\lambda_o$, allows the determination of $\Delta\lambda = (3.7 \pm 0.2) \times 10^{-4}$; considering the experimental errors this value is in accordance with that obtained in [26] and differs by 14% from those previously obtained in [26,36] ($(4.3 \pm 0.2) \times 10^{-4}$). This result reinforces the applicability of this procedure.

If the invariability of reflected integrated power of the sample with the dispersion is assumed it is possible to evaluate the half-width of the LiF single crystal diffraction patterns [26]. For a LiF (hkℓ) reflection, $\beta_{LiF\ hk\ell} = \beta_{hk\ell} \times (PI_{LiF\ hk\ell}/PI_{Ge\ 111})$ (Procedure I). Since

for damaged crystals a rectangular form is not always a good approximation for the BLP, in this paper the $\beta_{LiF\ hk\ell}$ from $B_{hk\ell}$ values are also evaluated (procedure II). Table I shows estimated values of the half-width of diffraction patterns of γ-irradiated LiF single crystals from procedures I and II; considering all approximations, the estimated error is of about 20%. A discrepancy (from 10 to 50%) between the two procedures is noted which increases as the β values increase. The high order reflections being the most affected by defects and experimental dispersion, the use of $\beta_{hk\ell}$ or $B_{hk\ell}$ in the $\beta_{LiF\ hk\ell}$ becomes critical. As a general tendency a decrease in β_{LiF} values with the increase of reflection order N is observed for all the samples, which would be expected at least for the less damaged samples. Different reflections present different behaviours as γ-dose increases (Fig. 4) but in general the alterations are not marked if the estimated error is considered. $\beta_{LiF\ 200}$ presents a decrease in its value for 50 MRad. $\beta_{LiF\ 111}$ increases at 100 MRad and as it becomes larger than $\beta_{Ge\ 111}$ (first crystal) it leads to a reduction of PI in the BLP resulting from the convolution of the two diffraction patterns; this can explain the decrease of PI_{111} at 100 MRad.

c) DIFFUSE X-RAY ANALYSIS

DXS analysis was done for six reflections. A typical sequence of the plots used is illustrated in Fig. 5, for the (220) reflection of LiF single crystal γ-irradiated at 0.5 MRad. The linear dependence between $|\vec{q}|$ and $|\delta\theta|$

has allowed the plotting of this parameter insted of $|\vec{q}|$.

Fig. 5a shows the log I vs. log$|\delta\theta|$ plot where the $\delta\theta$ values corresponding to $\theta>\theta_B$ and $\theta<\theta_B$ are identified. For (hkℓ) reflections of all the samples these plots have shown regions of linear behavior with different m slopes, as proposed in [22]. These m slope values, showed in Table 2, are not always integers, but vary from -1.2 to -3.0; similar results were obtained for silicon sample [29,26,27]. The decreasing of DXS intensity with q occurs in two different ranges: $q^{-1/2}$ - $q^{-1.9}$, which indicates that close to the defect the displacements are much larger than in an r^{-2} extrapolation of a long-range displacement field [25]; $q^{2.1}$ - $q^{3.0}$ which is a first indication of the q^{-4} dependence observed for even stronger defects [25]. The deviation from the q^{-2} low indicates also that the nearest neighbors of the clusters are strongly distorted [22]; this distortion is rather different for the heavily irradiated sample (the lowest m values) with a lighter displacement field in the core of the cluster. The intensity distribution of the DXS is different for the different studied reflections. This could be related to the presence of strain fields not spherically symmetric [9] as observed in [19]. It is also noted that the DXS relative intensity depends on the sites of the reciprocal lattice (Fig. 6) which is another evidence of the presence of non spherical symmetry [9].

Fig. 5b shows a typical plot of DXS intensity as function of $\ell n|\delta\theta|$ [24]. The behaviour of these plots, linear near the peak up to a q_{cr} (or the equivalent $|\delta\theta|_{cr}$) value, is related to strain fields internal and external to

the cluster [22]. From the q_o values the average sizes R_o of the aggregates are obtained, as shown in Table 2. The fitting of the straight line is closely dependent on the elimination of a few points very near to the Bragg peak, causing an uncertainty in the q_o value; this fact was taken into account when estimating the error in R_o (15%). Plots I vs. $1/|\delta\theta|^2$ (Fig.5c) were also employed to evaluate the parameter size of the cluster. The observed behaviour strongly suggests that the results are predominantly due to defect aggregates [29]. The straight lines with different slopes, as observed in other papers [26 to 30], allow the determination of the R values, from the knee points, showed in Table 2. Care was taken in varying successively the vertical and horizontal scales of the plots in order to better define the knee points. Each sample has presented clusters of several sizes. For each sample, each R value may be taken as the average value for a certain range of parameter size. Then, the set of R values may be taken as average values of the clusters for that sample. These R values will be referred to as prominent mean values. These prominent mean values are in accordance with the mean values R_o : for each sample and from each reflection, R_o could be taken as a representative value of the set of R values. Both parameter sizes have presented values varying from hundreds to thousands of angstroms. The largest clusters may be related to double spirals such as those observed in [33]. From all reflections, a decreasing in R_o and R values as the reflection order increases is noted. The high order reflections have presented the smallest half-

width values of diffraction pattern ($\beta_{LiF\ hk\ell}$) and are the most affected by defects. On the other hand, the diffraction patterns are particularly enlarged by instrumental dispersion, and give less information about the largest clusters. As a general tendency, R values increase with γ-dose; this can be observed from its maximum (R_M) and minimum (R_m) values. The largest R_o and R values are observed from all reflections of 50 MRad-sample. This is evident for R_m and R_m from (111), (200) and (311) reflections and for R_m from (220) and (222) reflections; the largest R values are obtained from (200) reflection.

To analyse the nature of the aggregates the asymmetries in DXS intensities are considered in terms of the θ-angles, since in reciprocal space when $\theta>\theta_B$ (or $\theta<\theta_B$) $\vec{q}$ is parallel (or antiparallel) to $\vec{h}$. The plotting of intensity on a logarithmic scale (log I vs. $\Delta\theta$), as shown in Fig.5d, gives qualitative evidence of the presence of DXS in BLP. Fig.6 allows the comparison of the DXS of some (hkℓ) reflections from the LiF samples (not all the experimental points are shown). Taking as reference the Bragg angle θ_B, these curves also attest the existence of anisotropies in the distribution of DXS intensity. Table 2 gives the predominant nature of the clusters in γ-irradiated LiF single crystals, from the different (hkℓ) reflections. At 0.5 MRad, some reflections do not showed marked asymmetries.

At low γ-dose the irradiation process has introduced clusters of a predominantly vacancy-type. With the increase of γ-dose, the interstitial-type tends to be

prevail; this is evident for 50 and 100 Rad γ-doses. The production of F centers in irradiated LiF crystals at low γ-dose and the presence of clusters of an interstitial-nature of higher γ-dose were admitted in [7] and substantial F center concentration is expected even at room temperature [37]. The presence of vacancy-type clusters due to low γ-doses in alkaline halogen was observed in KCℓ at 5 MRad [38] and X-ray irradiated NaCℓ single crystals have also presented vacancy clusters [19]. Clusters of interstitial atoms have been observed in LiF after γ-doses of 100 MRad [9] but with diameters of about seven lattice spacings. The increase of the irradiation dose favors clusters of an interstitial-nature and not of the vacancy-type, seems also in agreement with the higher mobility of interstitials than vacancies in irradiated alkaline halogen [39]. Clusters of an interstitial-nature preferentially distributed in <111> direction may be in accordance with ESR results about F_2^- molecules of H center being oriented in <111> direction [40].

Aggregation processes at about 50 MRad suggested by BLP results are in agreement with DXS results. At this γ-dose the largest values of the mean cluster size are observed from both analysis (R_o and R). A saturation of point defects aggregates seems to occur at γ-dose ≳ 50 MRad [8]. If the concentration c of aggregates remains constant but the aggregates grow, the Huang intensity increases proportionally to c^2 and the Stokes-Wilson intensity increases proportionally to c. But if the number of agglomerates also increases, both the Huang and the Stokes-Wilson intensity are then proportional to c. The increase of F-center concentration in very pure LiF

is proportional to the square root of the product of the intensity and the irradiation time in the range of about 1 to 500 MRad [2]. In the present case, the production of defects is dependent on the γ-dose and, as can be seen from DXS results, also their predominant nature, which means an inversion of the asymmetry. So, it is not easy to analyse the relative increasing of the DXS intensity as the γ-dose increases. From the majority of the reflections the DXS intensity presents a particular increase at 50 MRad. This could reinforce the presence of a coalescent process at this γ-dose. It is probable that some correlation exists between the behaviour of (111) BLP and interstitial clusters and (200) BLP parameters and vacany clusters.

CONCLUSION

The dispersion study from the half-width of a Bragg line profile taking into account the function $|tg\theta_{monoch.} - tg\theta_{sample}|$ has allowed a good anamorphosis. The linear coefficient of the adjusted straight line is in agreement with the half-width of the Ge monochromator crystal; from its angular coefficient the expected $\Delta\lambda/\lambda_o$ value was obtained. The half-width of the diffraction pattern ($\beta_{LiF\ hk\ell}$) of γ-irradiated LiF single crystals was estimated from the Bragg profile line parameters of the samples and of the monochromator crystal. Considering the evaluated error (about 20%) there is no marked increase in that half-width as the γ-dose increases. The

decreasing in $\beta_{LiF\ hk\ell}$ values for the high order reflections is evident. γ-irradiated LiF single crystals present complex alterations in the Bragg line profile, and not all of them may be understood in a simple way. The irradiation process has affected preferentially the (111) reflections, followed by the (200).

LiF single crystals irradiated at room temperature with ^{60}Co radiation at 0.5 to 100 MRad have presented clusters with mean parameter sizes from hundreds to thousands of angstroms. Each sample has presented several prominent average values. The clusters have showed a prevailing vacancy-nature at low γ-doses and interstitial-nature at high γ-doses. Interstitials produced by irradiation are stabilized in large clusters, probably distributed in <111> direction. The nature of the defects is dependent on the γ-dose. At least for large clusters, the strain fields are not spherically symmetrical.

At a dose of 50 MRad the aggregates of defects due to γ-irradiation tend to coalesce causing relatively more perfect regions to appear in the crystal. The increase of the γ-dose, producing a higher number of defects affect once more the partially acquired perfection. From 10 to 50 MRad there also occurs an inversion in the prevailing nature of clusters (from vacancy to interstitial).

ACKNOWLEDGEMENTS

The authors acknowledge the financial support of this work by FINEP and CNPq. They are grateful to L.Sanches for providing the irradiation of the samples. The authors also wish to thank Dr. L.Q. Amaral for reading the manuscript. One of the authors (PAF) thanks Prof. B.C. Brito Filho for useful discussions.

REFERENCES

[1] P. Durand, Y. Farge and M. Lambert, J. Phys. Chem. Sol. 30, 1353 (1969).

[2] Y. Farge, J. Phys. Chem. Sol. 30, 1375 (1969).

[3] E. Sonder and W.A. Sibley, in Point Defects in Solids, Crawford and Slifkin, Ed. (Plenum, N.York, 1972).

[4] V. Ausin and J.L. Alvarez Rivas, J. Phys. C5, 82 (1972).

[5] L.W. Hobbs, A.E. Hughes and D. Pooley, Proc. Roy. Soc. A332, 167 (1973).

[6] L.W. Hobbs, J. Phys. Coll. 34, C9-227 (1973).

[7] H. Peisl, H. Spalt and W. Waidelich, Phys. Stat. Sol. 23, K75 (1967).

[8] K. Guckelsberg and K. Neumaier, J. Phys. Chem. Sol. 36, 1353 (1975).

[9] H. Spalt, Z. Angew. Phys. 29, 269 (1970).

[10] W. Wagner, W. Waidelich and O. Wohofsky, J. Appl. Cryst. 7, 224 (1974).

[11] H. Spalt, J. Phys. Coll. 37, C7-507 (1976).

[12] C.A. Pimentel, PhD. Thesis, University of São Paulo, São Paulo (1972).

[13] C.A. Pimentel and S. Caticha-Ellis, J. Appl. Cryst. 10, 390 (1977).

[14] C.A. Pimentel and L.Q. Amaral, Nucl. Instr. & Meth. 148, 199 (1978).

[15] C.A. Pimentel and S. Caticha-Ellis, J. Microsc. Spectrosc. Electr. 4, 189 (1979).

[16] F. Sagastibelga and J.L.A. Rivas, J. Phys.C 4, 1873 (1981).

[17] V.L. Zefirova, E.V. Kolontsova and I.V. Telegina, Sov. Phys. Cryst. 20, 359 (1975).

[18] V.L. Zefirova, E.V. Kolontsova, G.S. Shdanov and V.P. Lutsenko, Sov. Phys. Cryst. 19, 686 (1975).

[19] E.V. Kolontsova and E.E. Kulago, Sov. Phys. Cryst. 20, 109 (1975).

[20] H. Peisl, J. Phys. Coll. 37, C7-47 (1976).

[21] P.A. Frugoli, Master Thesis, Univeristy of São Paulo, São Paulo (1981).

[22] P.H. Dederichs, J. Phys.F 3, 471 (1973).

[23] H. Peisl and H. Trinkauss, Comments on Sol. Stat. Phys. 5, 167 (1973).

[24] B.C. Larson and F.W. Young Jr., Z. Naturforsch. 28a, 626 (1973).

[25] P. Ehrhart and B. Schönfeld, Phys. Rev. 38, 3896 (1979).

[26] B.C. Brito-Filho, Master Thesis, University of São Paulo, São Paulo (1981).

[27] C.A. Pimentel and B.C. Brito-Filho, Submitted to publication.

[28] K. Lal, B.P. Singh and A.R. Verma, Acta Cryst. A35, 286 (1979).

[29] K. Lal and B.P. Singh, Acta Cryst. A36, 178 (1980).

[30] K. Lal and B.P. Singh, J. Crystal Growth 54, 493 (1981).

[31] J.R. Patel, J. Appl. Cryst. 8, 186 (1975).

[32] K. Lal and B.P. Singh, Sol. Stat. Comm. 22, 71 (1977).

[33] M.B. Ives and T.R. Ramachandran, J. Appl. Phys. 38, 2121 (1967).

[34] C.R.A. Catlow, J. Corish, K.M. Diller, P.W.M. Jacobs and M.J. Norgett, J. Phys. Coll. 37, C7-253 (1976).

[35] A.B. Lidiand, J. Phys. Coll. 34, C9-1 (1973).

[36] G. Brugen, Arkiv för Fysik 8, 391 (1954).

[37] S. Dannefaer, D.P. Kerr, G.W. Dean and B.G. Hogg, Can. J. Phys. 56, 1527 (1978).

[38] I.S. Braude and L.M. Rogozyanskaya, Sov. Phys. Sol. Stat. 20, 1317 (1978).

[39] F. Sonder, J. Phys. Coll. 34, C9-483 (1973).

[40] Y.H. Chu and R.L. Mieher, Phys. Rev. 118, 1311 (1969).

TABLE CAPTIONS

TABLE 1 - Half-width values of diffraction pattern β_{LiF} for γ-irradiated LiF single crystals obtained from β and B widths.

TABLE 2 - Characteristics of clusters in γ-irradiated LiF single crystals: mean cluster sizes R_o and R; interstitial (I), vacancy (V) nature or no marked asymmetry (NA). Slope values m.

FIGURE CAPTIONS

FIG. 1 - Variation of (hkℓ) Bragg profile parameters of irradiated LiF single crystals with the γ-dose: a) peak intensity PI; b) integrated intensity II.

FIG. 2 - Variation of (hkℓ) Bragg profile parameters of irradiated LiF single crystals with the γ-dose: a) integrated width B; b) width at half height β.

FIG. 3 - Influence of instrumental dispersion in the broadening of β as a function of: a) $1/\cos\theta_B$; b) $|tg\theta_{Ge\ 111} - tg\theta_{LiF\ hk\ell}|$.

FIG. 4 - Diffuse X-ray scattering curves of (hkℓ) reflections for LiF single crystals γ-irradiated at several doses.

FIG. 5 - Typical set of curves for DXS studies, referred to (220) reflection of γ-irradiated (0.5 MRad) LiF single crystals. a) log I vs. $\log|\delta\theta|$; b) I vs. $\ell n|\delta\theta|$; c) I vs. $1/|\delta\theta|^2$; d) log I vs. $\delta\theta$.

	β_{LiF} (sec. of arc)							
	from β				from B			
MRad / (hkℓ)	0.5	10	50	100	0.5	10	50	100
111	11	8	8	9	10	10	10	12
200	13	10	8	10	16	17	13	15
220	5	6	5	5	10	9	10	8
311	1.7	1.8	1.9	1.4	2.9	2.6	3.2	2.3
222	4.0	2.8	3.0	2.9	6	4.9	5	5
400	3.2	2.7	2.4	2.0	5	4.9	4.8	3.5

TABLE 1

	Slope (-m)				Mean Cluster Size (Å)								Nature of the Cluster			
					$R_o \times 10^3$				R (prominent values) $\times 10^2$							
MRad / (hkℓ)	0.5	10	50	100	0.5	10	50	100	0.5	10	50	100	0.5	10	50	100
(111)	1.8 2.5	2.6	1.3 2.9	2.8	4.5	5.0	7.0	5.1	7.6; 12; 19 ; 32; 53	11; 20; 26; 27; 37; 62	18; 29; 35; 87	17; 24; 27; 70	V	~I	I	I
(200)	1.3 1.7 2.2 2.4	1.5 2.5	1.5 2.5	1.0 1.7 2.1	3.6	3.5	4.0	3.3	16; 24; 25; 31; 39; 41	29; 30; 53	12; 46; 47	11; 21; 37;40	~V	I	I	I
(220)	1.7 2.6	1.6 3.0	1.7 2.9	1.5 2.2	1.7	1.6	2.1	1.7	3.3;4.1; 9.4; 12	3.7;4.8; 9.8; 16	3.7;5.0; 10; 17	5.4;6.0; 8.1; 14	N.A.	I	I	I
(311)	1.8 2.5	2.7	1.2 2.1	1.0 1.9	1.0	1.3	1.2	1.2	2.2; 4.6;7.9	3.2;8.4; 9.0; 15;	3.3;5.5; 8.2; 10; 13	3.0;8.6; 9.3	N.A.	~V	I	I
(222)	1.5 2.7	2.5 2.7	2.1 2.7	1.9	1.1	1.1	1.2	1.1	1.9;3.1; 4.7;5.6; 6.6;9.5; 12	1.8;2.6; 4.1;4.8; 7.9;8.5; 13	2.3;4.0; 8.0;8.4; 12; 14;	2.6;3.5; 6.7;7.1; 11;	V	~V	I	I
(400)	1.6 2.5	1.3 2.5	1.3 2.2	1.3 1.6 2.0	0.8	0.8	0.9	0.9	1.7;2.2; 2.7;3.6; 5.7;9.2	1.7;2.8; 3.8;4.6; 5.7;6.9 8.9;9.5	1.9;4.3; 5.2;7.2; 11	1.9;4.6; 7.6;7.8; 11; 12;	N.A.	I	I	I

TABLE 2

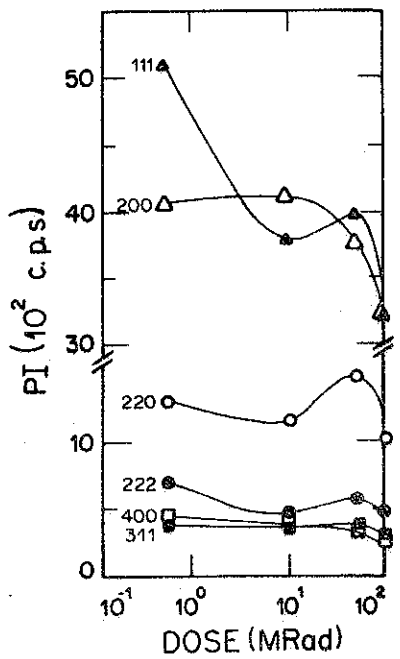

1a)

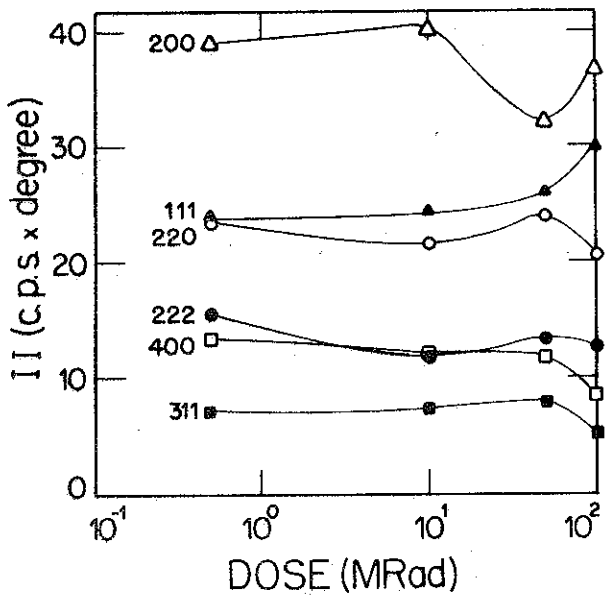

1b)

FIGURE 1

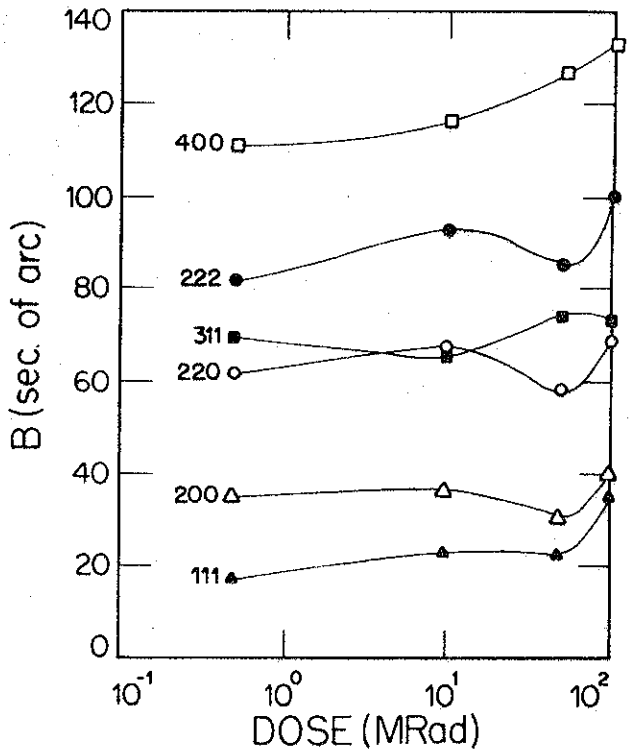

2a)

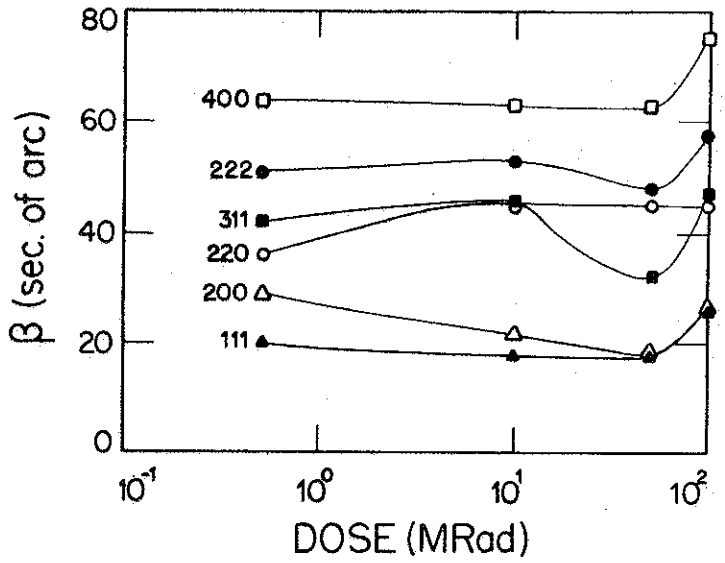

2b)

FIGURE 2

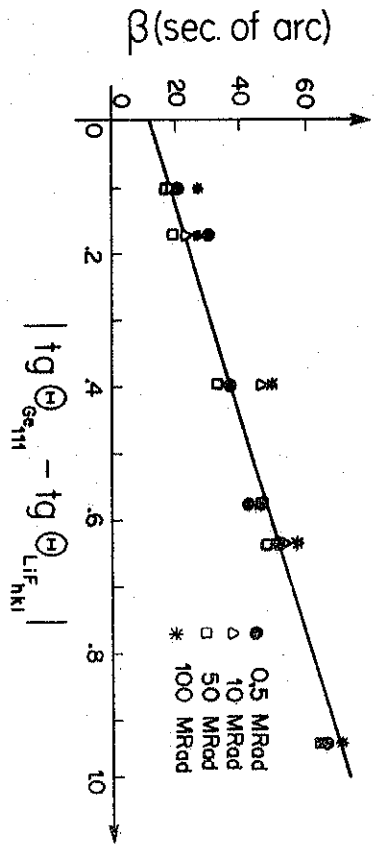

b)

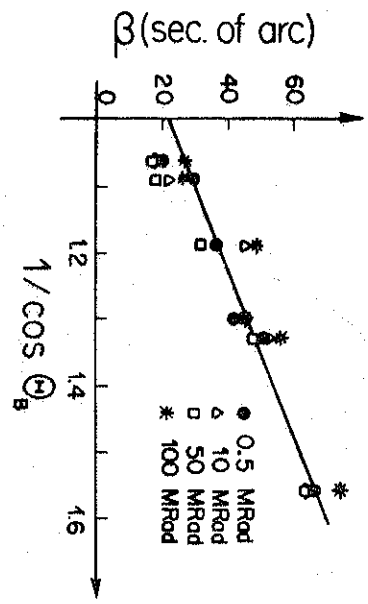

a)

FIGURE 3

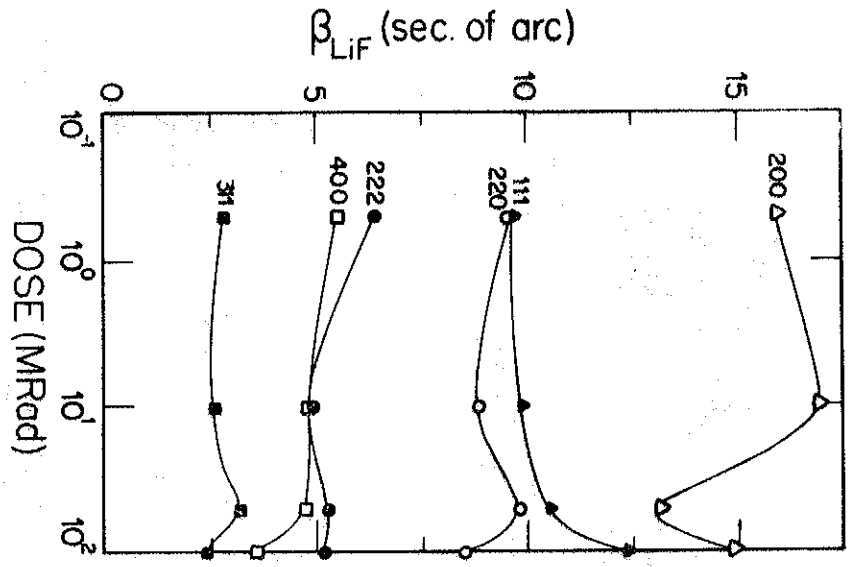

FIGURE 4

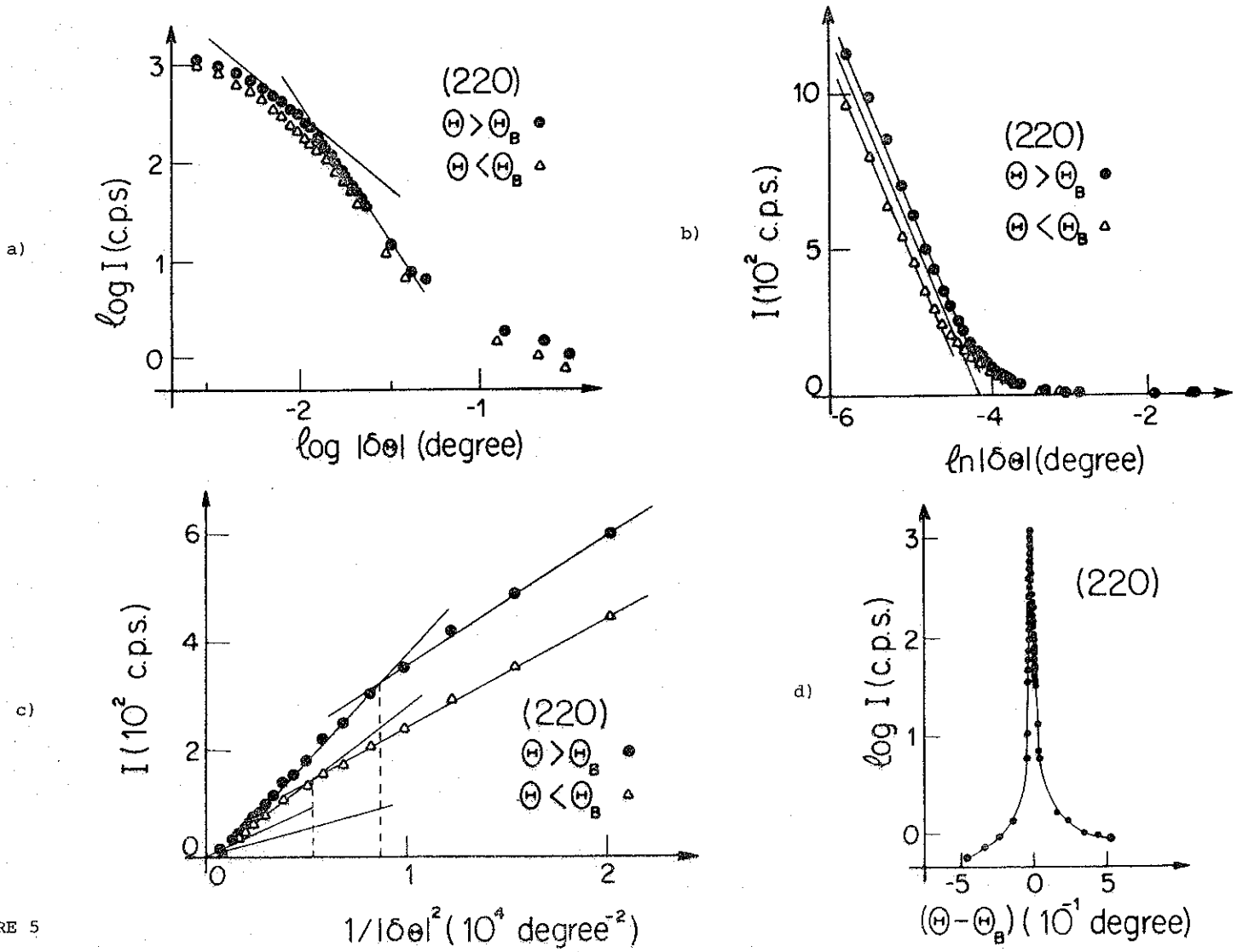

FIGURE 5

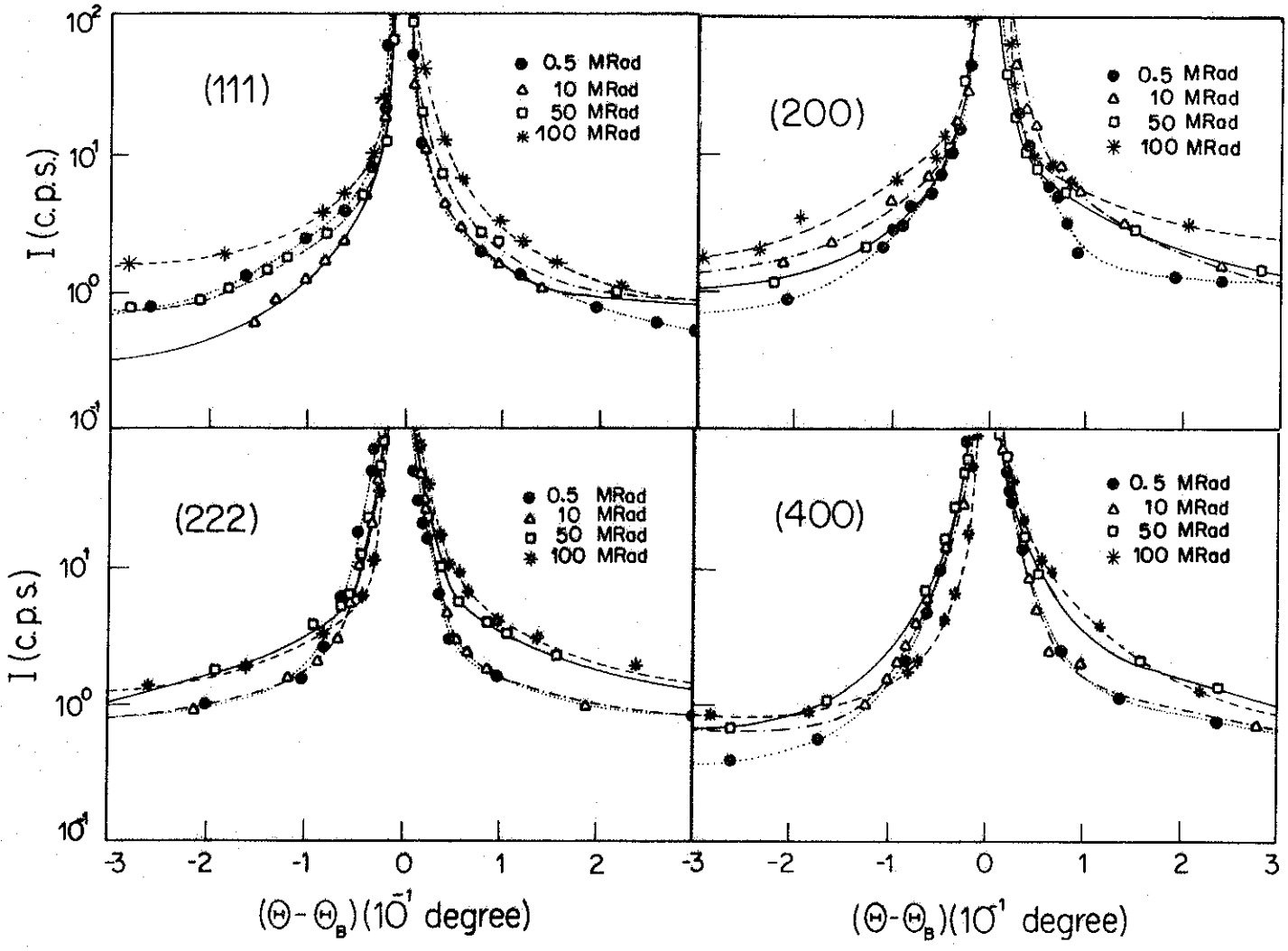
(111)
(200)
(222)
(400)
0.5 MRad
10 MRad
50 MRad
100 MRad
I (c.p.s.)
10^2
10^1
10^0
10^{-1}
-3
-2
-1
0
1
2
3
$(\Theta - \Theta_B)(10^{-1}$ degree)

FIGURE 6